AMB Express

RESEARCH

Open Access

Multi-omics analysis reveals the response mechanism of *Pichia kudriavzevii* to high-concentration lactic acid stress

Weiwei Li[1,2†], Ning Wang[1,2†], Jia Zheng[3], Ahmed H. El-Sappah[4,5], Huibo Luo[1,2], Weiming Jiang[6], Rongfei Wang[1,2], Linjuan Li[1,2], Puyu Zhang[1,2], Dalong Liao[1,2], Hong Wang[3], Hui Zhu[1,2*] and Muhammad A. Mehmood[1,2*]

Abstract

Pichia kudriavzevii tolerance mechanisms are not well understood, even though strong-flavor Baijiu fermentation places a heavy burden on yeast metabolism due to the accumulation of lactic acid (LA). This study utilized growth kinetics, electron mi-croscopy, antioxidant tests, and integrated metabolomic-transcriptomic studies to an-alyze strain Y2-1, which was isolated from Baijiu pit yellow water. Y2-1 showed a de-layed biphasic growth pattern and could withstand up to 80 g/L of LA. It appears that morphological adaptation plays a role in stress resistance, as scanning electron mi-croscopy showed that cells elongated significantly at high LA levels. Enrichment in pyruvate metabolism, glutathione metabolism, and ABC transporter pathways was among the 1,125 differentially expressed genes and 817 different metabolites found using multi-omics analysis. In order to maintain membrane integrity, ergosterol homeo-stasis, and mitochondrial function, mechanistically speaking, LA tolerance entailed three strategies: (i) activating pyruvate metabolism, which channeled lactate into energy metabolism and mitigated proton imbalance; (ii) enhancing the glutathione antioxidant system, which included spermidine synthase upregulation and improved ROS scavenging and intracellular pH buffering; and (iii) induction of ABC transporters (SNQ2, ABCB7). Molecular insights into yeast acid tolerance and a foundation for creating robust strains to boost Baijiu fermentation efficiency are offered by these findings, which indicate a metabolic-transport-linked defense strategy.

Keywords *Pichia kudriavzevii*, Lactic acid stress, Multi-omics analysis, Baijiu fermentation

[†]Weiwei Li and Ning Wang contributed equally to this work.

*Correspondence:
Hui Zhu
zhuhuiwn@outlook.com
Muhammad A. Mehmood
nibgian@gmail.com
[1]Sichuan Province Engineering Technology Research Center of Liquor-Making Grains, Sichuan University of Science and Engineering, Yibin 644000, China
[2]Yibin Sichuan University of Science and Engineering Industrial Technology Research Institute, Yibin 644000, China
[3]Wuliangye Group Co., Ltd, Yibin 644007, China
[4]College of Agriculture, Forestry, and Food Engineering, Yibin University, Yibin 644000, China
[5]Genetics Department, Faculty of Agriculture, Zagazig University, Zagazig, Egypt
[6]Wenchuan Yingxiu People Tea Co. Ltd, Aba 623000, China

Introduction

Organic acids serve multiple functions as essential elements influencing the flavor character of Baijiu during fermentation. Conventional research has predominantly concentrated on the direct effects of four principal organic acids—acetic acid, lactic acid, butyric acid, and hexanoic acid—on sensory attributes, frequently underappreciating the role of lactic acid (LA) (Wang et al. 2022; Zhu et al. 2025a). Recent research suggests that suitable concentrations of LA not only alleviate the sensory impacts of ethanol and provide a balanced sourness (Li et al. 2019a, b), but also function as aroma enhancers that markedly increase the volatility of ethyl hexanoate—a distinctive scent constituent of robust-flavored Baijiu (Zhang et al. 2022). In a typical multi-microbial fermentation system, organic acids in Baijiu fermentation function as both flavor precursors and ecological regulators: short-chain acids (e.g., lactic and acetic acids) directly impart cheesy and sour notes, while long-chain fatty acids mitigate the volatility of ethyl esters, thus modulating flavor expression; concurrently (Wang et al. 2019, 2022; Liu et al. 2023), lactic and acetic acids specifically promote the proliferation of functional pit mud microbiota (such as *Clostridium sensu stricto* and *acid-producing Clostridia*), optimizing microbial community structure (Chai et al. 2021; Qian et al. 2021). The dynamic equilibrium of organic acids significantly regulates fermentation in both directions: excessive accumulation alters cellular proton gradients, resulting in membrane damage, inactivation of genetic material, and enzyme inhibition, which ultimately hinders microbial metabolism (Giannattasio et al. 2005; Jeong et al. 2008). In the manufacture of strong-flavor Baijiu, the concentration gradient of lactic acid in the fermented broth (yellow water) directly influences the metabolic activity of yeast. Moderate amounts refine microbial interactions, while excessive concentrations induce cellular stress, leading to variable fermentation efficiency and product inconsistencies (Zhou et al. 2019; Ying et al. 2023; Zhu et al. 2025b). Consequently, unraveling the tolerance mechanisms of yeast to lactic acid has emerged as a critical scientific concern for refining conventional brewing procedures and obtaining accurate flavor management.

P. kudriavzevii is a dominant species within the genus *Pichia* during Baijiu fermentation (Jiang et al. 2019), serving a dual function in flavor development and fermentation safety management. This yeast generates taste precursors, including higher alcohols and volatile acids (Liu et al. 2017), while simultaneously diminishing the buildup of harmful chemicals such as ethyl carbamate, thereby improving product safety (Du et al. 2018). The exceptional stress tolerance provides ecological benefits in the intricate brewing environment: research indicates that specific strains (e.g., grape-derived isolate NG7) can endure up to 4% lactic acid at 50 °C (Park et al. 2018). Strains derived from Baijiu fermentation must further acclimatize to various stresses, including high acidity, increased ethanol levels, and interspecies competition. The yeast's response to lactic acid is strain-specific and concentration-dependent: adaptive metabolic pathways may be activated under mild acid conditions, whereas high amounts result in growth suppression. Subsequent research suggests that *P. kudriavzevii* preserves intracellular homeostasis via the dynamic control of transmembrane transport, antioxidant defenses, and energy metabolism networks; however, its specific tolerance mechanisms have yet to be clarified entirely (Stratford et al. 2013). Integrated metabolomic and transcriptome analysis yields precise insights into gene–metabolite interaction networks, facilitating a systematic exploration of the production and regulation of metabolic processes (Li et al. 2019a, b).This methodology addresses the shortcomings of single-omics investigations and provides a more accurate interpretation of the expression patterns and pathways associated with essential functioning genes (Ying et al. 2023). Research indicates that *Saccharomyces cerevisiae* reacts to lactic acid stress in acidic environments by adjusting its antioxidant capacity, intracellular glycerol concentrations, and metabolic pathways (Jiang et al. 2023; Zhang et al. 2023a, b). Acid stress triggers the formation of reactive oxygen species (ROS) in yeast cells, activating antioxidant defense mechanisms such as the glutathione metabolic pathway and increasing superoxide dismutase (SOD) activity (Zhang et al. 2023a, b). While prior research has substantially elucidated the adaptation processes of *P. kudriavzevii* in low-lactate setting (Du et al. 2022), its precise tolerance mechanisms under high lactic acid stress are still inadequately investigated. The morphological changes in *P. kudriavzevii* under elevated lactic acid stress, together with the dynamic modifications and regulatory networks of essential intracellular metabolic pathways, remain inadequately characterized.

This study examined the tolerance mechanism of the *P. kudriavzevii* strain Y2-1, isolated from the fermentation broth (yellow water) of strong-flavor Baijiu, to elevated lactic acid stress by conducting a thorough analysis of its growth characteristics, cellular morphology, antioxidant capacity, metabolomic profile, and transcriptomic responses at different lactic acid concentrations. Initially, we evaluated the growth curves and biomass variations of the strain under varying lactic acid conditions, then used scanning electron microscopy to examine morphological changes and measure total antioxidant capacity (T-AOC). Additionally, by untargeted metabolomics and transcriptome sequencing, we examined alterations in metabolites and gene expression under elevated lactic acid stress and identified critical metabolic pathways through KEGG enrichment analysis. The results offer

multi-omics data for comprehending the adaptation mechanisms of yeast to high acid stress and establish a theoretical basis for improving the stress resistance of brewing microorganisms.

Materials and methods

Strain, culture medium, and culture conditions

The yeast strain *P. kudriavzevii* Y2-1, isolated from the yellow water of strong-flavor Baijiu, was preserved in the China General Microbiological Culture Collection Center (CGMCC), CGMCC No.33254. All yeast strains were stored at − 80 °C in YPD broth supplemented with glycerol. For subsequent seed culture preparation, the strains were first revived by incubating on YPD agar plates at 37 °C for 24 h.

Growth curve measurement and Gompertz model fitting

YPD liquid medium was acidified using different concentrations of lactic acid: 0 g/L (pH = 6.50), 40 g/L (pH = 2.1), 80 g/L (pH = 1.96), and 120 g/L (pH = 1.87), with three replicates per group. The growth dynamics of the strain were monitored using a MicroScreen HT real-time microbial growth analysis system (Gerering, Tianjin, China). A yeast seed suspension at a concentration of 1.0×10^6CFU/mL was inoculated at 5% (v/v) into a 48-well plate, with each well containing a total volume of 1000 µL. The plate was incubated at 37 °C with shaking at 180 rpm, and the OD_{600} was automatically measured every 10 min until the late plateau phase was reached. Growth curves were plotted with fermentation time (h) on the x-axis and OD_{600} on the y-axis.

To quantitatively characterize the growth kinetics under different lactic acid concentrations, the growth curves were fitted to the Gompertz model using nonlinear regression. Fitting was performed using the nonlinear regression (growth curve) module of GraphPad Prism 9.0. The kinetic parameters (Y_M, Y_0, K) for each treatment group were estimated by an iterative method, and the inflection time $(1/K)$ and goodness of fit (R^2) were calculated. Three biological replicates were used for each group, and the results are expressed as the fitted value ± 95% confidence interval.

Effect of lactic acid on yeast morphology

Yeast morphological changes were examined with minor modifications based on a previously described method (Wang et al. 2024). Briefly, a seed suspension of 1.0×10^6CFU/mL was inoculated at 5% (v/v) into 100 mL of YPD liquid medium containing different lactic acid concentrations (0, 40, and 80 g/L) in 500 mL conical flasks. Cultures were incubated at 37 °C with shaking at 180 rpm until the mid-to-late logarithmic phase was reached. Cells were harvested by centrifugation at 3000 r/min for 3 min.

The harvested cells were washed three times with 0.1 M phosphate-buffered saline (PBS, pH 7.0) and fixed with 2.5% (v/v) glutaraldehyde at 4 °C for 24 h. After discarding the fixative, the cells were rinsed three times with 0.1 M PBS (pH 7.0), each for 15 min. The samples were then dehydrated stepwise in an ethanol series (50%, 60%, 70%, 80%, 90%, and 100%), each for 15–20 min. Subsequently, the dehydrated samples were transferred to a mixture of ethanol and isoamyl acetate (v: v = 1:1) for approximately 30 min, followed by pure isoamyl acetate for 1 h. Finally, the samples were critical-point dried using liquid CO_2, sputter-coated with gold-palladium, and observed under a scanning electron microscope (SEM, VEGA3 TESCAN), Cell lengths were then measured using image analysis software (ImageJ).

Determination of total antioxidant capacity (T-AOC)

Yeast seed culture was inoculated at 5% (v/v) into 50 mL of YPD liquid medium containing 0, 40, or 80 g/L lactic acid and incubated at 37 °C with shaking at 180 rpm until the mid-logarithmic phase. Cells were collected by centrifugation at 3000 r/min for 3 min. The total antioxidant capacity (T-AOC) was determined using the FRAP method. A standard curve was established, and the T-AOC of the samples was calculated according to the instructions of the Total Antioxidant Capacity Assay Kit (FRAP Method).

Untargeted metabolomics analysis

Based on the comprehensive analysis of growth phenotypes and antioxidant responses, high concentrations of lactic acid were found to trigger more intense oxidative stress and systemic regulatory processes. To maximize the capture of key genes and metabolic pathway changes related to lactic acid tolerance, the control group (C) and the high-concentration lactic acid group (LH) were selected for subsequent transcriptomic and metabolomic analyses, aiming to further elucidate the tolerance mechanism of *P. kudriavzevii* to high-concentration lactic acid stress. Beijing Novogene Co., Ltd, measured metabolomic bioinformatics data.

Briefly, metabolite extraction was first performed for LC–MS detection. Liquid chromatography (Thermo Fisher) and mass spectrometry (Thermo Fisher) were used for identification in both positive (ESI+) and negative (ESI–) ion modes. The raw data files were imported and processed using CD 3.3 software for preliminary screening based on retention time and mass-to-charge ratio parameters of each metabolite. Peak area correction was performed using the first quality control (QC) sample as a reference. Identified metabolites were annotated using public databases, including HMDB, LipidMaps, and KEGG. For multivariate statistical analysis, the metabolomics data processing software metaX was

used to perform principal component analysis (PCA) and partial least squares-discriminant analysis (PLS-DA), from which VIP values for each metabolite were derived. For univariate analysis, a t-test was applied to calculate the statistical significance (P value) of each metabolite between the two groups, and the fold change (FC) was computed. Differential metabolites were screened with default thresholds of VIP > 1, *P* value < 0.05, and FC ≥ 2 or FC ≤ 0.5.

Illumina transcriptome sequencing

RNA extraction, sequencing, and bioinformatic analysis were conducted by Beijing Novogene Co., Ltd. Cells for RNA extraction were collected from three biological replicates each of the high-concentration lactic acid group (LH) and the control group (C). Total RNA was extracted using Trizol reagent according to the manufacturer' 's instructions (Invitrogen, Carlsbad, CA, USA). RNA quality and quantity were assessed, libraries were constructed, and pairedend sequencing (150 bp) was performed on the Illumina HiSeq X Ten platform. Differential expression analysis between the two comparison groups was performed using the DESeq2 R package (v1.20.0). Enrichment of differentially expressed genes in KEGG pathways was analyzed using the cluster-Profiler R package (v3.8.1).

Integrated metabolomic and transcriptomic analysis

KEGG pathways enriched with metabolites were selected for correlation analysis with corresponding genes. All differentially expressed genes and metabolites were mapped to the KEGG pathway database to identify shared pathways, thereby determining the key biochemical and signal transduction pathways commonly involved. Enrichment of pathways common to both differential metabolites and genes was further performed via the iPath website, and metabolic pathway maps were generated based on the enrichment results.

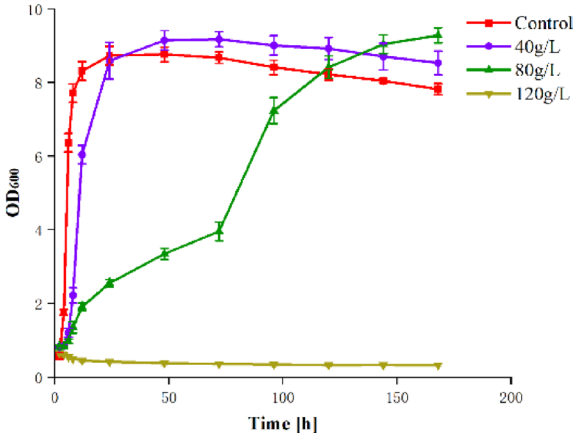

Fig. 1 Biomass of *P. kudriavzevii* Y2-1 during fermentation under lactic acid stress at different concentrations (40 g/L, 80 g/L, and 120 g/L) (Control)

Data processing

All experimental data are presented as the mean ± standard deviation (SD) of three replicates. Statistical differences among groups were assessed using one-way analysis of variance (ANOVA) followed by Tukey's multiple comparisons test in GraphPad Prism 9.0. A *P* value < 0.05 was considered statistically significant, and *P* < 0.01 was considered highly significant.

Results

Analysis of lactic acid resistance in acid-tolerant yeast

The growth curves of *P. kudriavzevii* Y2-1 under different lactic acid concentrations were fitted using the Gompertz model. Compared to the control group (0 g/L), both the 40 g/L and 80 g/L treatments increased the maximum asymptote (YM). The 80 g/L group exhibited the highest YM (11.57); however, its rate constant (K) was significantly lower (0.01583) than that of the control (0.3826), and its inflection time (1/K) was as long as 63.19. This indicates that while this concentration enhances the final biomass, it results in extremely slow growth and a significantly prolonged lag phase. Although the 40 g/L group had a very low starting value (Y0 = 0.0004), its relatively high K value (0.2703) suggests rapid growth from a low initial point. In contrast, the 120 g/L treatment severely inhibited growth, with a YM of only 0.3397, and exhibited low K values (0.03881) and a poorer goodness of fit (R^2 = 0.8517), alongside wide confidence intervals for the parameters, suggesting a potential toxic effect at this concentration. The high R^2 values (> 0.97) for all treatments except 120 g/L indicate that the Gompertz model accurately describes the growth dynamics. In conclusion, lactic acid concentrations of 40 and 80 g/L enhance the final growth peak at the cost of extending the lag phase and reducing the growth rate, whereas a concentration of 120 g/L completely suppresses the growth of the strain (Fig.1).

Morphological changes of yeast under different lactic acid concentrations

Figure 2 illustrates that the control cells displayed a complete oval morphology. As evidenced by the quantified cell length data, Following treatment with low-concentration lactic acid (40 g/L), *P. kudriavzevii* Y2-1 cells exhibited modest morphological alterations, demonstrating a propensity for elongation, The cell length was 1.61 times that of the control group. In high-concentration lactic acid (80 g/L), most cells showed a fully elongated shape, The cell length was 2.49 times that of the control group. The results indicate that lactic acid significantly elongates *P. kudriavzevii* cells, with the extent of morphological

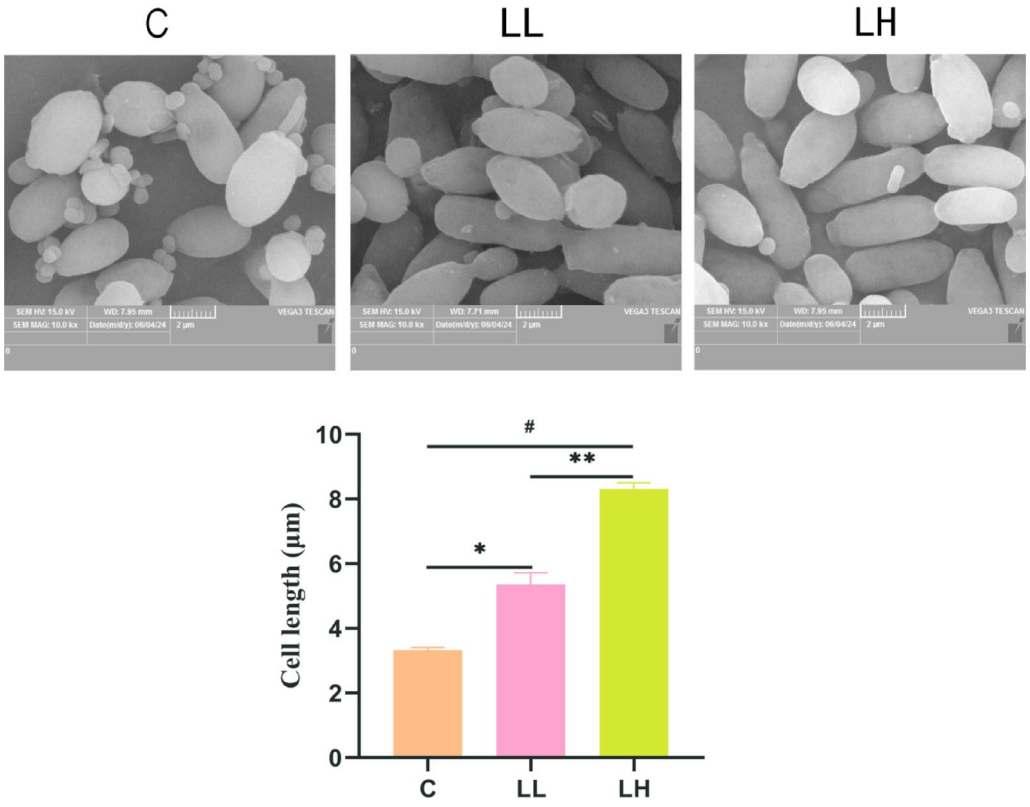

Fig. 2 SEM morphology and cell length analysis of *P. kudriavzevii* Y2-1 under different lactic acid concentrations. "C" indicates negative control, "LL" indicates 40 g/L, and "LH" indicates 80 g/L

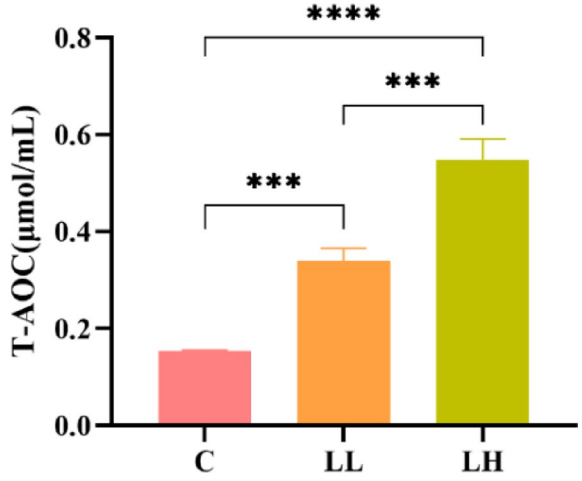

Fig. 3 Changes in the total antioxidant capacity of yeast under lactic acid stress at different concentrations. "C" indicates negative control, "LL" indicates 40 g/L, and "LH" indicates 80 g/L

change accelerating as lactic acid concentration rises. This suggests that strain Y2-1 may acclimatize to elevated lactic acid stress via morphological alterations.

Changes in total antioxidant capacity of yeast under lactic acid stress

The total antioxidant capacity (T-AOC) of yeast cells subjected to varying doses of lactic acid was assessed using the T-AOC Assay Kit, and a Fe^{2+} standard curve was generated. The standard curve was established as $y = 10.633x + 0.0632$ ($R^2 = 0.9996$), utilized for calculating the T-AOC of the samples. The findings indicated that the T-AOC values of yeast subjected to 40 g/L and 80 g/L lactic acid stress were 2.27 times and 3.67 times greater, respectively, than those of the control group. This suggests that the antioxidant ability of strain Y2-1 progressively enhances with increasing lactic acid concentration (Fig. 3).

Dynamic changes in the metabolic profile of yeast under high-concentration lactic acid stress

PCA results showed a clear separation between the metabolic profiles of the two groups, with the cumulative contribution rate of PC1 and PC2 reaching 85.89% (Fig. 4A). PLS-DA (Fig. 4B) further confirmed significant intergroup differences. The model was validated as reliable (Fig. 4C) with permutation test intercepts of R^2 = 0.89 and Q^2 = −2.00. The volcano plot (Fig. 4D) revealed a total of 817 differential metabolites, of which 361 were upregulated and 455 were down-regulated. Further

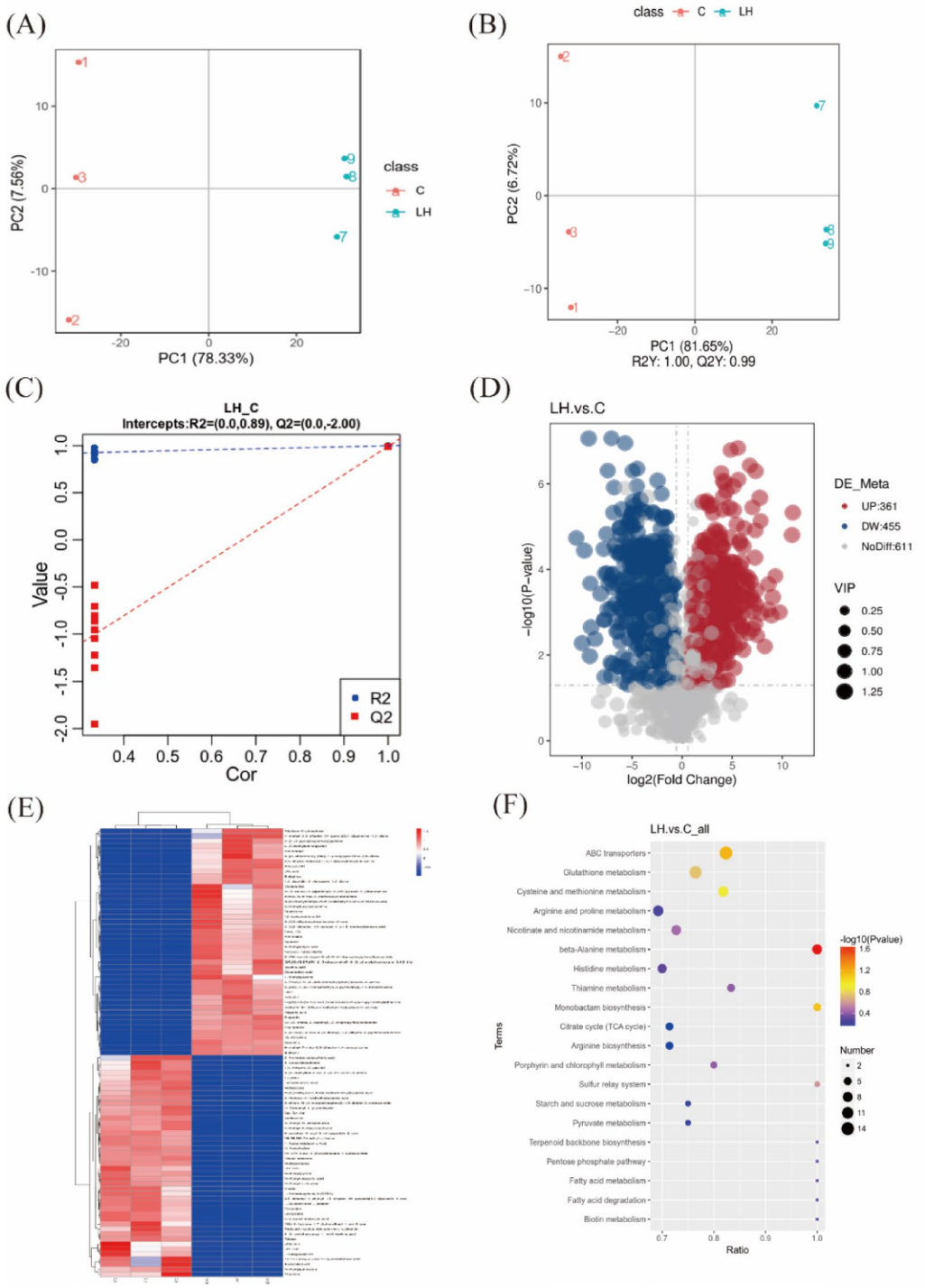

Fig. 4 Changes in the metabolic profile of *P. kudriavzevii* before and after treatment with high concentrations of lactic acid based on untargeted metabolomic sequencing. **A** Principal component analysis (PCA) score plot. **B** Partial least squares-discriminant analysis (PLS-DA) plot. **C** Vali-dation plot of the PLS-DA model. **D** Volcano plot of differential metabolites. **E** Heatmap of clustered differential metabolites. **F** Bubble plot of KEGG pathways. "C" indicates negative control, "LH" indicates 80 g/L)

Table 1 Genes related to pyruvate metabolism

Enzyme	GeneID	log2FoldChange
Phosphoenolpyruvate carboxykinase	C5L36_0A03670	3.96
L-lactate dehydrogenase	C5L36_0C03700	2.24
Acetyl-CoA hydrolase	C5L36_0A09950	1.84
Malate dehydrogenase	C5L36_0E04340	1.83
Pyruvate dehydrogenase	C5L36_0B09180	1.40
Pyruvic carboxylase	C5L36_0A02450	1.73
Pyruvate dehydrogenase complex component	C5L36_0B12580	1.06
Malate synthase	C5L36_0E02440	1.79
Aldehyde dehydrogenase	C5L36_0C08090	1.72
D-lactate dehydrogenase	C5L36_0B11920	2.35
Pyruvate kinase	C5L36_0A06840	-2.71
Acetyl-CoA carboxylase	C5L36_0C09260	-2.57
Homocitrate synthase	C5L36_0C01170	-2.00
Acetyl-coenzyme A synthetase	C5L36_0C06790	2.65
Homocitrate synthase	C5L36_0D05690	-1.27
Acetyl-coenzyme A synthetase	C5L36_0C05470	-1.16
2-isopropylmalate synthase	C5L36_0D05520	-1.70
Pyruvate dehydrogenase	C5L36_0B02890	1.02
Lactoylglutathione lyase	C5L36_0A01040	-1.01
Acetyl-CoA acetyltransferase	C5L36_0B09210	-1.01
lactate dehydrogenase	C5L36_0B09360	1.27
K(+)-activated acetaldehyde dehydrogenase	C5L36_0E03210	1.62
D-lactate dehydrogenase	C5L36_0B11920	2.35

screening (VIP > 1.25, $P < 0.01$, FC ≥ 10 or ≤ 0.2) identified 89 key differential metabolites (Table 1), including heterocyclic compounds, organic acids and derivatives, lipids, nucleoside analogues, and other categories. Clustering heatmap (Fig. 4E) showed that 45 metabolites were upregulated and 44 were down-regulated. Pathway enrichment analysis (Fig. 4F) indicated that β-alanine metabolism, ABC transporters, glutathione metabolism, and nicotinate and nicotinamide metabolism are core metabolic pathways in the response of *P. kudriavzevii* to lactic acid stress.

Transcriptomic analysis of yeast under high-concentration lactic acid stress

Transcriptomic sequencing generated a total of 275,334,208 raw reads, with 264,956,718 clean reads retained after quality control. Principal component analysis (PCA) demonstrated good reproducibility within groups and significant differences between groups, supporting subsequent analyses (Fig. 5A). Using the criteria $|Log_2FC| \geq 1$ *and* $Padj \leq 0.05$*, a total of 1,125 differentially expressed genes (DEGs) were identified, including 444 up-regulated and 681 down-regulated genes (Fig. 5B). KEGG enrichment analysis (Fig. 5C and D) showed that the DEGs were significantly enriched in pathways such as biosynthesis of secondary metabolites (107 genes), oxidative phosphorylation (53 genes), and amino acid biosynthesis. These results indicate that P. kudriavzevii enhances its tolerance to high-concentration lactic acid by regulating the expression of genes related to secondary metabolism and energy metabolism.*

Integrated metabolomic and transcriptomic analysis

Particular features at the gene expression and metabolite levels were derived from transcriptomic and metabolomic data. Transcription and metabolism are not independent processes in biological systems (Zhou et al. 2019). Joint KEGG pathway analysis of metabolites and genes (Fig. 6A and B) revealed that pathways significantly down-regulated following high-concentration lactic acid treatment were predominantly associated with amino acid biosynthesis (e.g., valine, leucine, isoleucine, arginine, cysteine, and methi-onine metabolism), secondary metabolite biosynthesis, energy metabolism (e.g., pentose phosphate pathway, pyruvate metabolism, TCA cycle), and fatty acid metabolism. Conversely, markedly upregulated pathways encompassed antioxidant response (e.g., glutathione metabolism), energy metabolism (oxidative phosphorylation, carbon me-tabolism), nucleotide metabolism (purine and pyrimidine metabolism), cofactor synthesis (e.g., riboflavin and thiamine metabolism), and specific amino acid metabolisms (e.g., tryptophan and phenylalanine metabolism).

To clarify the regulatory mechanisms between gene expression and metabolites, we mapped and investigated various metabolic pathways strongly enriched in KEGG categories using integrated omics data. As illustrated in Fig. 6C, genes associated with lactate breakdown were markedly up-regulated in strain Y2-1 under high-concentration lactic acid stress relative to the control Table 1). The expression of the L-lactate dehydrogenase gene (EC: 1.1.2.3) was upregulated by 2.24-fold, which is crucial for catalyzing the conversion of L-lactate to pyruvate. The expression levels of genes encoding pyruvate dehydrogenase (EC: 1.2.4.1), malate synthase (EC: 2.3.3.9), malate dehydrogenase (EC: 1.1.1.37), and phosphoenolpyruvate carboxykinase (EC: 4.1.1.49) were upregulated by factors of 1.01, 1.79, 1.82, and 3.96, respectively. Pyruvate is initially transformed into acetyl-CoA by pyruvate dehydrogenase (EC: 1.2.4.1); thereafter, acetyl-CoA is enzymatically changed by malate synthase (EC: 2.3.3.9) and malate dehydrogenase (EC: 1.1.1.37) to yield (S)-malate and oxaloacetate. Ultimately, one molecule of oxaloacetate is subsequently coupled with phosphoenolpyruvate by the action of phosphoenolpyruvate carboxykinase (EC: 4.1.1.49) to create pyruvate, while another molecule enters the TCA cycle.

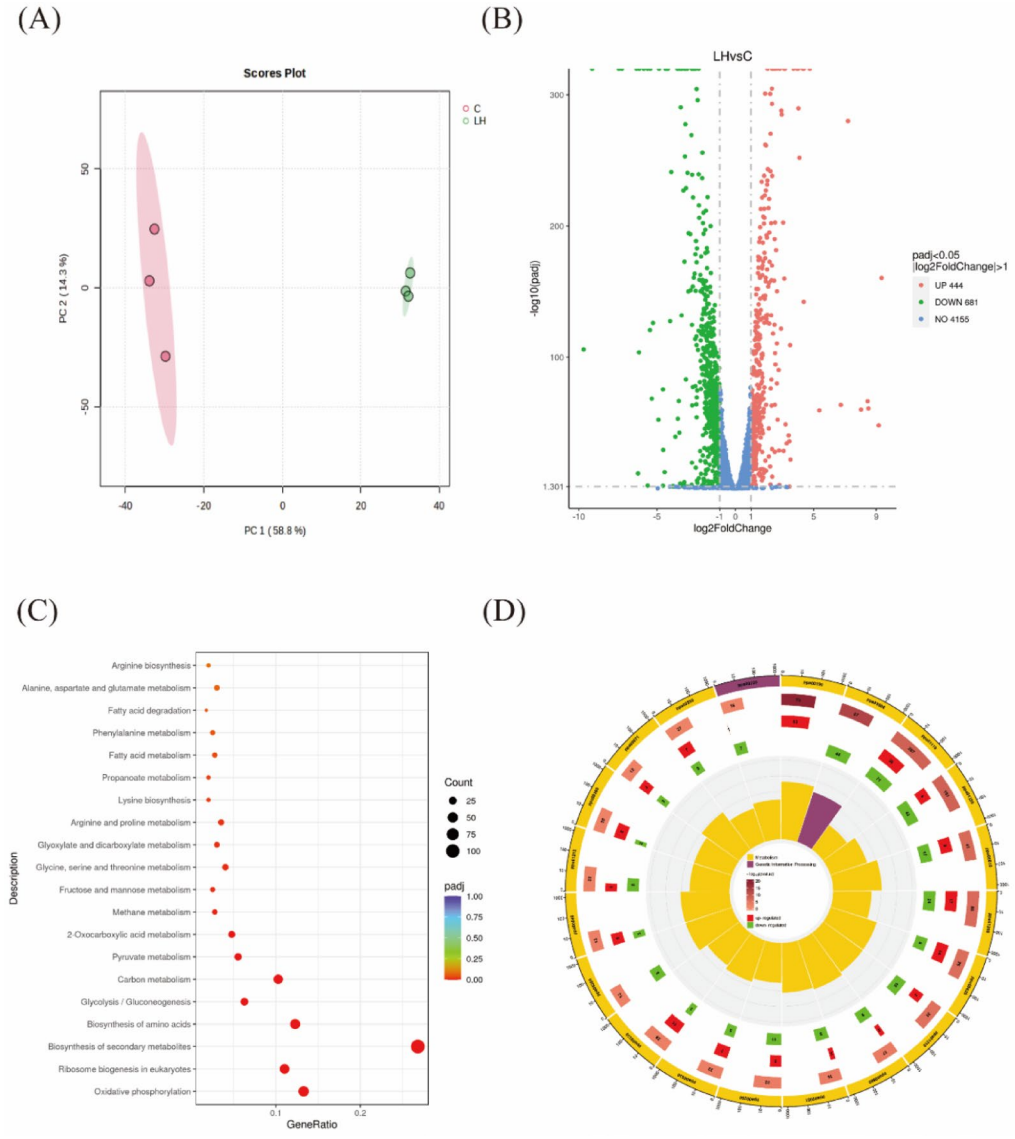

Fig. 5 Transcriptomic analysis. **A** Principal component analysis (PCA) score plot. **B** Volcano plot of differentially expressed genes. **C** Bubble plot of KEGG enrichment analysis. **D** Circle plot of KEGG enrichment analysis. "C" indicates negative control, "LH" indicates 80 g/L)

The expression levels of genes encoding spermidine synthase (EC: 2.5.1.16) and ornithine decarboxylase (EC: 4.1.1.17) in the glutathione (GSH) metabolic pathway were considerably up-regulated by 1.25-fold and 1.19-fold, respectively (Table 2). These enzymes function synergistically to transform intermediates from the arginine biosynthesis route into glutathione, thereby augmenting cellular antioxidant potential. Subsequent study demonstrated a substantial enhancement of intracellular GSH synthesis in low pH settings (Fig. 6C).

Under high-concentration lactic acid stress, the expression of genes encoding NADH dehydrogenase (EC: 1.6.5.3) and NADH oxidase (EC: 1.6.99.3) was considerably up-regulated by 2.11-fold and 2.02-fold, respectively (Table 3). The collaborative function of these enzymes efficiently transforms intracellular NADH into NAD^+ and H^+, preserving cellular redox equilibrium. Simultaneously, the expression of genes producing CoQ-cytochrome c reductase (EC: 1.10.2.2) and cytochrome c oxidase (EC: 1.9.3.1) was markedly upregulated, attaining 11.62-fold and 2.04-fold of the control levels, respectively. These enzymes collectively engage in the electron transport chain, transporting H^+ to the mitochondrial intermembrane space through the actions of Complexes III and IV, ultimately facilitating ATP synthesis via Complex V (mitochondrial ATP synthase, EC: 3.6.3.14), which catalyzes the phosphorylation of ADP while releasing H^+.

In summary, high-concentration lactic acid treatment significantly impacts the metabolic network of *P. kudriavzevii*, down-regulating various anabolic pathways while

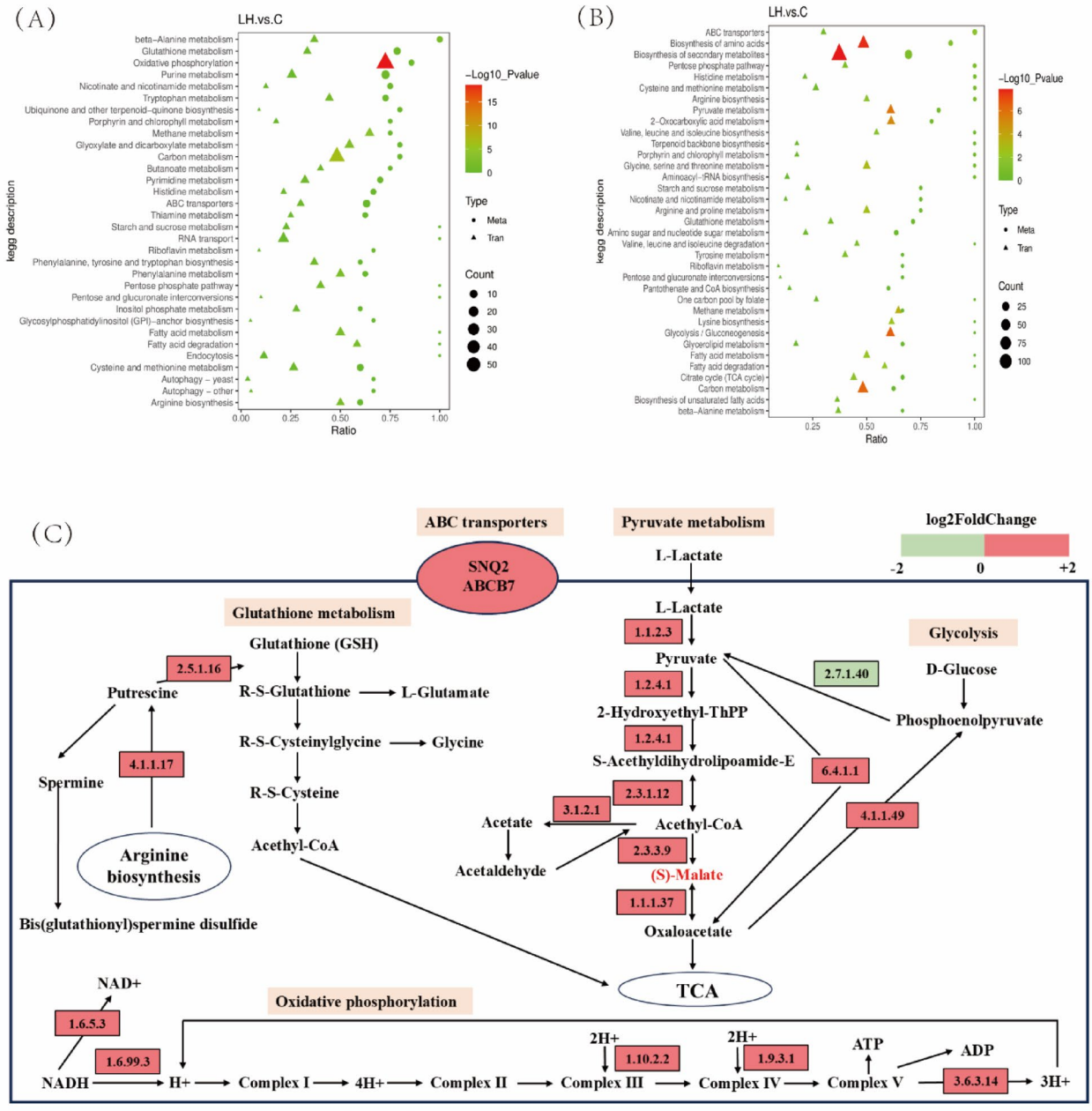

Fig. 6 Integrated analysis. **A** Bubble plot of KEGG enrichment analysis of differentially expressed genes and differential metabolites in positive ion mode. **B** Bubble plot of KEGG enrichment analysis of differentially expressed genes and differential metabolites in negative ion mode. **C** Proposed response pathway of *P. kudriavzevii* Y2-1 to high-concentration lactic acid stress

up-regulating those associated with energy production, stress response, and nucleotide metabolism, indicating that lactic acid reconfigures metabolic processes to affect cellular function.

Discussion

This study thoroughly examined the growth, morphology, antioxidant capacity, metabolomics, and transcriptomics of *P. kudriavzevii* Y2-1 under varying concen-trations of lactic acid stress, elucidating its tolerance mechanisms and adaptive responses under high-lactate conditions. The findings demonstrate that the strain had a brief adaptation phase and fast proliferation at low lactic acid

Table 2 Genes related to glutathione metabolism

Enzyme	GeneID	log2FoldChange
Glucose-6-phosphate dehydrogenase	C5L36_0A11100	− 3.43
6-phosphogluconate dehydrogenase	C5L36_0C07630	− 1.77
Ribonucleotide reductase	C5L36_0A10760	− 2.07
Mitochondrial peroxiredoxin	C5L36_0E00560	1.86
Ribonucleotide reductase	C5L36_0A12560	− 1.20
Spermidine synthase	C5L36_0C06150	1.26
Ornithine decarboxylase	C5L36_0C09900	1.20

Table 3 Genes related to oxidative phosphorylation

Enzyme	GeneID	log2FoldChange
Mitochondrial ATP synthase	C5L36_0C01220	1.90
NADH-ubiquinone oxidoreductase	C5L36_0E01197	2.03
	C5L36_0B06150	1.44
	C5L36_0D02015	1.73
	C5L36_0D01770	1.44
	C5L36_0B00140	1.32
	C5L36_0A03310	1.43
	C5L36_0D06100	1.40
	C5L36_0C06880	1.29
	C5L36_0C01360	1.36
	C5L36_0C05850	1.16
	C5L36_0C02225	1.18
	C5L36_0C06665	1.06
NADH dehydrogenase	C5L36_0B11815	2.11
	C5L36_0E00715	2.03
cytochrome reductase	C5L36_0D00980	1.62
cytochrome c reductase	C5L36_0D01450	1.60
	C5L36_0B03540	1.57
	C5L36_0B04280	1.35
	C5L36_0B03180	1.29
	C5L36_0E01710	1.70
Cytochrome c oxidase	C5L36_0A09510	1.96
	C5L36_0B06050	1.88
	C5L36_0B06090	1.48
	C5L36_0A08450	1.77
	C5L36_0A08440	1.71
	C5L36_0D05180	2.05
	C5L36_0D01820	1.43
	C5L36_0C02290	1.36
	C5L36_0A07530	1.44
	C5L36_0E04590	1.07
ATP synthase	C5L36_0B08710	1.78
	C5L36_0A01530	1.85
	C5L36_0C10810	1.52
	C5L36_0B06570	1.46
	C5L36_0C09830	2.47
	C5L36_0B08000	1.48
	C5L36_0B01110	1.85
	C5L36_0A06200	2.16

concentration (40 g/L), whereas its growth rate markedly diminished at elevated concentrations (80 g/L). Nonetheless, it ensured survival by extending the adaptation phase and regulating metabolic pathways.

Morphological research indicated that elevated lactic acid stress caused significant alterations in yeast cell morphology, potentially linked to osmoregulation mechanisms. This morphological adjustment, characterized by cellular elongation, may increase the surface area-to-volume ratio, thereby facilitating proton efflux, enhancing the diffusion of hazardous compounds, and improving the distribution density of surface ABC transporters. In contrast, a previous study reported that lactic acid stress had no significant effect on the colony and cell morphology of *P. kudriavzevii* (strain PY1) (Pan et al. 2024). However, using strain Y2-1, our study observed a distinct morphological response: exposure to high concentrations of lactic acid (80 g/L) induced pronounced cellular elongation. This discrepancy suggests that the morphological response to lactic acid stress may be strain-dependent within the *P. kudriavzevii* species. The elongation observed in Y2-1 could represent a specific adaptive mechanism to mitigate high lactic acid stress, potentially by altering the surface-to-volume ratio for nutrient uptake or waste export. The measurement of antioxidant capacity revealed that the total antioxidant capacity (T-AOC) of the yeast markedly increased with elevated lactic acid concentrations. Under lactic acid stress of 40 g/L and 80 g/L, total antioxidant capacity (T-AOC) rose by 2.27-fold and 3.67-fold, respectively, demonstrating that the yeast augments its antioxidant defense system to mitigate lactate-induced oxidative stress.

Integrated metabolomic and transcriptome investigations demonstrated that pathways including oxidative phosphorylation, pyruvate metabolism, and glutathione metabolism are essential to the lactic acid tolerance mechanism in yeast. Previous investigations have demonstrated that cells exposed to low levels of weak acid have time to adapt, but fast exposure to high concentrations causes distinct stress responses (Giannattasio et al. 2005). Consistent with prior research, *P. kudriavzevii* destroys lactate via the pyruvate metabolic route (Deng et al. 2020). Under elevated lactate stress, strain Y2-1 markedly stimulated the pyruvate metabolism pathway, evidenced by the coordinated overexpression of critical enzymes, including L-lactate dehydrogenase (LldD), pyruvate dehydrogenase, and malate synthase (Lin et al. 2018). LldD facilitates the transformation of lactate into pyruvate and is important to this process. This regulatory network enables lactate metabolism through two pathways: first, lactate is transformed into pyruvate by LldD, subsequently entering the TCA cycle for energy generation; second, oxaloacetate supports gluconeogenesis via phosphoenolpyruvate carboxykinase, creating a closed

loop in carbon metabolic flux (Fig. 6C). This mechanism alleviates proton imbalance due to intracellular lactate accumulation and sustains efficient ATP synthesis through the interplay of the TCA cycle and oxidative phosphorylation (e.g., upregulation of genes encoding NADH dehydrogenase and CoQ-cytochrome c reductase), thereby supplying energy for stress responses.

Lactate accumulation has several detrimental effects on cells, including intracellular acidification, anion accumulation, membrane disruption, disturbed amino acid transport, increased turgor pressure, ATP depletion, ROS accumulation, metabolic dysregulation, and metal chelation (Peetermans et al. 2021). In response to acid stress-induced ROS in-crease, cells enhance the synthesis of glutathione (GSH), a crucial ROS scavenger (Nugroho et al. 2015). As a principal antioxidant, GSH neutralizes lipid peroxides through glutathione peroxidase to preserve membrane integrity, while its thiol groups regulate intracellular protons to reduce acid toxicity (Fan et al. 2025). Moreover, GSH increase reduces intracellular proton concentration, relieving acid-induced damage and consequently boosting yeast cell adaptability and survival in acidic environments (Zhu et al. 2022).

Oxidative phosphorylation not only produces the majority of ATP necessary for higher animals and plants to sustain life but also contributes to the establishment and maintenance of metabolic equilibrium. This study demonstrated substantial activation of oxidative phosphorylation-related genes (e.g., NADH oxidase, cytochrome c oxidase), which not only optimized proton gradient efficacy and ATP production in the electron transport chain but also preserved coenzyme equilibrium by enhancing NAD+ regeneration, thus averting metabolic stagnation caused by redox imbalance. These reactions provide crucial energy and successfully sustain cellular homeostasis by modulating proton gradients and redox states, hence improving yeast tolerance to elevated lactate stress.

Lactate tolerance requires not only amino acid homeostasis but also metal cation homeostasis. Genes associated with iron metabolism were significantly impacted by lactate stress (Kawahata et al. 2006). ABCB7 mitigates ROS accumulation through the regulation of iron-sulfur cluster transport (Kim et al. 2020), whereas plasma membrane ABC transporters such SNQ2 dynamically modulate ergosterol homeostasis, thereby preserving membrane integrity and reducing the dissipation of transmembrane potential. This is indicated by reduced membrane permeability and stabilized electrochemical gradients under chemical stress (Godinho et al. 2018). This study demonstrated a substantial upregulation of both SNQ2 and ABCB7. The systemic enhancement of this protein family augments the efficiency of the efflux system by actively transporting intracellular toxic substances, such as metabolic byproducts and exogenous xenobiotics, for detoxification, a mechanism notably evident in carboxylic acid stress responses in *Saccharomyces cerevisiae* (Yi et al. 2015; Du et al. 2022). ABC transporters, the most significant family of transmembrane transporters in living organisms, establish a complex molecular barrier that contributes to cellular defense, metabolic equilibrium, and environmental adaptation, owing to their substrate diversity and functional versatility (Wang et al. 2016). Compared to the unidirectional detoxifying function of ScSnq2 in *S. cerevisiae* (Godinho et al. 2018), strain Y2-1 demonstrated more complicated regulatory network characteristics in transporter expression, showing evolutionary adaptive differences in acid stress responses among yeast species.

Conclusions

The multi-omics research shows that *P. kudriavzevii* Y2-1 has a unified tolerance mechanism that allows it to survive the intense lactic acid loads that are common in Baijiu fermentations. In terms of phenotype, this strain can withstand lactic acid concentrations up to 80 g L^{-1}, grows slowly but steadily, and exhibits the telltale signs of cell elongation. What's more, its antioxidant capacity grows in direct correlation with her stress levels. From a mechanistic standpoint, integrated metabolomic-transcriptomic analyses have shown a metabolic-transport coupling that maintains energy homeostasis and limits acid toxicity. This coupling involves the following steps: (i) activating a carbon flux centered on pyruvate, which includes L-lactate dehydrogenase and downstream TCA/gluconeogenic nodes; (ii) strengthening the glutathione axis, which improves intracellular pH buffering and ROS scavenging; and (iii) upregulation of ABC transport modules, such as SNQ2 and ABCB7, supports membrane integrity, iron-sulfur homeostasis, and efflux of toxicants, stabilizing mitochondrial function, and the transmembrane potential. All of these parts work together to create a buffer zone that redirects biosynthesis away from anabolism and toward energy production and stress reduction. These discoveries do more than only shed light on yeast acid tolerance at the systems level; they also identify potential targets for rational strain engineering and process control, including carbon flux nodes, glutathione/polyamine metabolism, and specific ABC transporters. The use of these levers provides a molecular foundation for choosing or creating more robust starters and optimizing fermentation conditions, which in turn improves Baijiu's resilience, flavor consistency, and production efficiency.

Acknowledgements

The authors would like to especially thank Yuting Zhang and Yang Li for their assistance with the preparation of samples for scanning electron microscopy,

and Pei Meng, Meina Liu, and Hongjun Hu for their work on the pretreatment of samples for omics sequencing in this study.

Author contributions

W.W.L. and N.W. contributed equally to this work. W.W.L. and H.Z. conceived the study. N.W. and J.Z. designed the study and wrote the first version of the manuscript. H.W.,and H.B.L. participated in its design, co-ordination and performed the statistical analysis. L.J.L. and W.M.J. performed the validation work. D.L.L., M.H.E. and M.A.M. collected and analyzed the raw data. P.Y.Z., N.W. and R.F.W. revised the manuscript. H.Z.* (Corresponding author) is responsible for this study, participated in its design and coordination and help to draft the manuscript. All authors have read and approved the final manuscript.

Funding

This work was funded by grants from the Wuliangye Industry University research cooperation project (grant no. CXY2021ZR009), Yibin Science and Technology Program (Grant NO. 2024SF015), Yibin Agricultural Science and Technology Innovation Project (grant number H72313004), Sichuan Province Engineering Technology Research Center of Liquor-Making Grains (grant number 2022-04), Liquor Making Biotechnology and Intelligent Manufacturing of Key Laboratory of China National Light Industry (grant number 2023-02), 2024 Provincial Financial Rural Revitalization Transfer Payment Fund Park Construction Project, Yibin City Agricultural and Rural Bureau.

Conflict of interest: The authors declare that the research was conducted in the absence of any commercial or financial relationships that could be construed as a potential conflict of interest.

Data availability: The raw sequence data reported in this paper were deposited in the genome sequence archive (Genomics, Proteomics & Bioinformatics 2017) in the National Genomics. Data Center (Nucleic Acids Res 2021), China National Center for Bioinformation/Beijing Institute of Genomics, Chinese Academy of Sciences, under accession number CRA009003 and are publicly accessible at https://bigd.big.ac.cn/gsa.

Data availability

The raw sequence data reported in this paper were deposited in the genome sequence archive (Genomics, Proteomics & Bioinformatics 2017) in the National Genomics. Data Center (Nucleic Acids Res 2021), China National Center for Bioinformation/Beijing Institute of Genomics, Chinese Academy of Sciences, under accession number CRA009003 and are publicly accessible at [https://bigd.big.ac.cn/gsa](https:/bigd.big.ac.cn/gsa) .

Declarations

Competing interests

The authors declare no competing interests.

Received: 19 December 2025 / Accepted: 13 March 2026
Published online: 29 March 2026

References

Chai LJ, Qian W, Zhong XZ, Zhang XJ, Lu ZM, Zhang SY, Wang ST, Shen CH, Shi JS, Xu Z (2021) Mining the factors driving the evolution of the pit mud microbiome under the impact of long-term production of strong-flavor Baijiu. App Environ Microb 87:e0088521. https://doi.org/10.1128/AEM.00885-21

Deng N, Du H, Xu Y (2020) Cooperative response of *Pichia kudriavzevii* and *Saccharomyces cerevisiae* to lactic acid stress in Baijiu fermentation. J Agric Food Chem 68:4903–4911. https://doi.org/10.1021/acs.jafc.9b08052

Du H, Song Z, Xu Y (2018) Ethyl carbamate formation regulated by *lactic acid bacteria* and *Nonconventional Yeasts*. Liquor J Agric Food Chem 66:387–392. https://doi.org/10.1021/acs.jafc.7b05034. Solid-State Fermentation of Chinese Moutai-Flavor

Du H, Fu Y, Deng N, Xu Y (2022) Transcriptional profiling reveals adaptive response and tolerance to lactic acid stress in *Pichia kudriavzevii*. Foods 11:2725. https://doi.org/10.3390/foods11182725

Fan H, Wan Y, Huang Y, Yuan J, Fan J, Kou Y, Yu X, Pan Y, Huang D, Fu G (2025) Breeding of lactic acid-tolerant *Saccharomyces cerevisiae* based on atmospheric and room temperature plasma technology and automatic high-throughput microbial microdroplet culture system. Food Microbiol 128:104717. https://doi.org/10.1016/j.fm.2024.104717

Giannattasio S, Guaragnella N, Corte-Real M, Passarella S, Marra E (2005) Acid stress adaptation protects *Saccharomyces cerevisiae* from acetic acid-induced programmed cell death. Gene 354:93–98. https://doi.org/10.1016/j.gene.2005.03.030

Godinho CP, Dias PJ, Ponçot E, Sá-Correia I (2018) The Paralogous genes PDR18 and SNQ2, encoding multidrug resistance ABC transporters, derive from a recent duplication event, PDR18 being specific to the *Saccharomyces* genus. Front Genet 9:476. https://doi.org/10.3389/fgene.2018.00476

Jeong KC, Hung KF, Baumler DJ, Byrd JJ, Kaspar CW (2008) Acid stress damage of DNA is prevented by Dps binding in *Escherichia coli* O157:H7. BMC Microbiol 8:181. https://doi.org/10.1186/1471-2180-8-181

Jiang J, Liu Y, Li H, Yang Q, Wu Q, Chen S, Tang J, Xu Y (2019) Modeling and regulation of higher alcohol production through the combined effects of the C/N ratio and microbial interaction. J Agric Food Chem 67:10694–10701. https://doi.org/10.1021/acs.jafc.9b04545

Jiang L, Lu Y, Ma Y, Liu Z, He Q (2023) Comprehensive investigation on volatile and non-volatile metabolites in low-salt doubanjiang with different fermentation methods. Food Chem 413:135588. https://doi.org/10.1016/j.foodchem

Kawahata M, Masaki K, Fujii T, Iefuji H (2006) Yeast genes involved in response to lactic acid and acetic acid: acidic conditions caused by the organic acids in Saccharomyces cerevisiae cultures induce expression of intracellular metal metabolism genes regulated by Aft1p. Fems Yeast Res 6:924–936. https://doi.org/10.1111/j.1567-1364.2006.00089.x

Kim JY, Kim JK, Kim H (2020) ABCB7 simultaneously regulates apoptotic and non-apoptotic cell death by modulating mitochondrial ROS and HIF1α-driven NFκB signaling. Oncogene 39:1969–1982. https://doi.org/10.1038/s41388-019-1118-6

Li C, Xu Y, Li L, Yang X, Wang Y (2019a) Acid stress induces cross-protection for cadmium tolerance of multi-stress-tolerant *Pichia kudriavzevii* by regulating cadmium transport and antioxidant defense system. J Hazard Mater 366:151–159. https://doi.org/10.1016/j.jhazmat.2018.11.101

Li H, Qin D, Wu Z, Sun B, Sun X, Huang M, Sun J, Zheng F (2019b) Characterization of key aroma compounds in Chinese Guojing sesame-flavor Baijiu by means of molecular sensory science. Food Chem 284:100–107. https://doi.org/10.1016/j.foodchem.2019.01.102

Lin YC, Cornell WC, Jo J, Price-Whelan A, Dietrich LEP (2018) The *Pseudomonas aeruginosa* complement of lactate dehydrogenases enables use of d- and l-lactate and metabolic cross-feeding. mBio 9:e00961–e00918. https://doi.org/10.1128/mBio.00961-18

Liu PL, Xiong XM, Wang S, Miao LH (2017) Population dynamics and metabolite analysis of yeasts involved in a Chinese miscellaneous-flavor liquor fermentation. Ann Microbiol 67:553–565. https://doi.org/10.1007/s13213-017-1286-y

Liu QR, Lin XL, Lu ZM, Chai LJ, Wang ST, Shi JS, Zhang SY, Shen CH, Zhang XJ, Xu ZH (2023) Influence on the volatilization of ethyl esters: nonnegligible role of long-chain fatty acids on Baijiu flavor via intermolecular interaction. Food Chem 436:137731–137731. https://doi.org/10.1016/j.foodchem.2023.137731

Nugroho RH, Yoshikawa K, Shimizu H (2015) Metabolomic analysis of acid stress response in *Saccharomyces cerevisiae*. J Biosci Bioeng 120:396–404. https://doi.org/10.1016/j.jbiosc.2015.02.011

Pan WS, Lin XF, Yang XP, Xu Y, Hou X (2024) Effect of lactic acid stress on the solid-state fermentation characteristics of Pichia kudriavzevii. Sci Technol Food Ind 45(4):116–122. https://doi.org/10.13386/j.issn1002-0306.2023050193

Park HJ, Bae JH, Ko HJ, Lee SH, Sung BH, Han JI, Sohn JH (2018) Low-pH production of D-lactic acid using newly isolated acid tolerant yeast *Pichia kudriavzevii NG7*. Biotechnol Bioeng 115:2232–2242. https://doi.org/10.1002/bit.26745

Peetermans A, Foulquié-Moreno MR, Thevelein JM (2021) Mechanisms underlying lactic acid tolerance and its influence on lactic acid production in *Saccharomyces cerevisiae*. Microb Cell 8:111–130. https://doi.org/10.15698/mic2021.06.751

Qian W, Lu ZM, Chai LJ, Zhang XJ, Li Q, Wang ST, Shen CH, Shi JS, Xu ZH (2021) Cooperation within the microbial consortia of fermented grains and pit mud drives organic acid synthesis in strong-flavor Baijiu production. Food Res Int 147:110449–110449. https://doi.org/10.1016/j.foodres.2021.110449

Stratford M, Steels H, Nebe-von-Caron G, Novodvorska M, Hayer K, Archer DB (2013) Extreme resistance to weak-acid preservatives in the spoilage yeast *Zygosaccharomyces bailii*. Int J Food Microbiol 166:126–134. https://doi.org/10.1016/j.ijfoodmicro.2013.06.025

Wang M, Deng WW, Zhang ZZ, Yu O (2016) Engineering an ABC transporter for enhancing resistance to caffeine in *Saccharomyces cerevisiae*. J Agric Food Chem 64:7973–7978. https://doi.org/10.1021/acs.jafc.6b03980

Wang MY, Yang JG, Zhao QS, Zhang KZ, Su C (2019) Research progress on flavor compounds and microorganisms of maotai flavor Baijiu. J Food Sci 84:6–18. https://doi.org/10.1111/1750-3841

Wang G, Jing S, Wang X, Zheng F, Li H, Sun B, Li Z (2022) Evaluation of the perceptual interaction among ester odorants and nonvolatile organic acids in Baijiu by GC-MS, GC-O, odor threshold, and sensory analysis. J Agric Food Chem 70:13987–13995. https://doi.org/10.1021/acs.jafc.2c04321

Wang L, Jang SS, Li DH, Sun CY (2024) Combined transcriptomics and metabolomics analysis reveals the antifungal activity and mechanism of *Enterococcus faecium* cell-free supernatant against Alternaria alternata. Food Biosci 57:103442. https://doi.org/10.1016/J.FBIO.2023.103442

Yi X, Gu H, Gao Q, Liu ZL, Bao J (2015) Transcriptome analysis of Zymomonas *mobilis ZM4* reveals mechanisms of tolerance and detoxification of phenolic aldehyde inhibitors from lignocellulose pretreatment. Biotechnol Biofuels 8:153. https://doi.org/10.1186/s13068-015-0333-9

Ying L, Wei HZ, Dinakaran E, Hai XL, Dan DJ, Xiao YW, Ying W (2023) Metabolome and transcriptome analysis reveals molecular mechanisms of watermelon under salt stress. Environ Exp Bot 206. https://doi.org/10.1016/j.envexpbot.2022.105200

Zhang Q, Shi J, Wang Y, Zhu T, Huang M, Ye H, Wei J, Wu J, Sun J, Li H (2022) Research on interaction regularities and mechanisms between lactic acid and aroma compounds of Baijiu. Food Chem 397:133765–133765. https://doi.org/10.1016/j.foodchem.2022.133765

Zhang J, Deng J, Zheng J, Ma Y, Luo H, Luo X, Hou C, Huo D (2023a) Organic acid-induced triple fluorescent emission carbon quantum dots identification of distilled liquor. Food Chem 422:136080. https://doi.org/10.1016/j.foodchem.2023.136080

Zhang Y, Xu Y, Li N, Liu X, Ma Y, Yang SY, Luo H, Hou C, Huo D (2023b) An ultrasensitive electrochemical sensor based on antimonene simultaneously detect multiple heavy metal ions in food samples. Food Chem 421:136131. https://doi.org/10.1016/j.foodchem.2023.136131

Zhou S, Chen J, Lai Y, Yin G, Chen P, Pennerman KK, Yan H, Wu B, Zhang H, Yi X, Wang C, Fu M, Zhang X, Huang L, Ma X, Peng Y, Yan Y, Nie G, Liu L (2019) Integrative analysis of metabolome and transcriptome reveals anthocyanins biosynthesis regulation in grass species Pennisetum purpureum. Ind Crop Prod 138:111470–111470. https://doi.org/10.1016/j.indcrop.2019.111470

Zhu H, Lan C, Zhao D, Wang N, Du D, Luo H, Lu H, Peng Z, Wang Y, Qiao Z, Huang Y, Sun B (2022) Wuliangye Baijiu but not ethanol reduces cardiovascular disease risks in a zebrafish thrombosis model. NPJ Sci Food 6:55. https://doi.org/10.1038/s41538-022-00170-2

Zhu H, Li L, Ma Y, Luo H, El-Sappah AH, Liu Y, Sun X, Pan S, Mehmood MA, Sun Y (2025a) Volatilomics and lipidomics revealed flavoring mechanism in baijiu brewed from diverse Sorghum varieties. Food Chem 485:144503. https://doi.org/10.1016/j.foodchem.2025.144503

Zhu H, Li Q, Sappah AHE, Sun Y, Liu Y, Pan S, Zhu K, Sun X, Xiong T, Luo H, Wu T, Li L, Ma Y, Wang N (2025b) Influence of two sorghum varieties on metabolic factors, microbial community, and flavor component precursors of strong-flavor Baijiu Zaopei. Food Chem 474:143079. https://doi.org/10.1016/j.foodchem.2025.143079

Publisher's note